Received: 25 September 2020 | Revised: 19 February 2021 | Accepted: 19 March 2021

High Voltage

DOI: 10.1049/hve2.12097

ORIGINAL RESEARCH PAPER

Analysis of influence of a novel inductive fault current limiter on the circuit breaker in 500 kV power system

Qiang Tang[1] | Shenli Jia[1] | Yanzhe Zhang[1] | Shixin Xiu[1] | Wenxiong Mo[2] | Yong Wang[2] | Haibo Su[2]

[1]Department of Electrical Engineering, Xi'an Jiaotong University, China

[2]Test and Research Institute of Guangzhou Power Supply Company Ltd., Guangzhou, China

Correspondence

Shenli Jia, Department of Electrical Engineering, Xi'an Jiaotong University, China.
Email: sljia@mail.xjtu.edu.cn

Associate Editor: Jiaxin Yuan

Funding information

National Key Research and Development Program of China, Grant/Award Number: 2018YFB0904300

Abstract

A contribution to the engineering application of a proposed 500 kV fault current limiter (FCL) is presented. A new type of FCL composed of a highly coupled split reactor (HCSR) and fast switches is proposed. When the circuit breaker (CB) in series with the FCL in the 500 kV power system interrupts the limited fault current, the rate of rise of the recovery voltage (RRRV) reaches a value much higher than the rated value. Based on a simplified equivalent single-phase circuit, the influence of the new FCL on the interruption procedure of the CB is simulated and discussed. The simulation results show that the high RRRV is caused by high-frequency resonant oscillations between the HCSR and its parasite capacitance. Analysis indicates that when the reactance of the FCL is close to the short circuit reactance of the system, the RRRV will reach the highest value. To solve this issue, we proposed installing a shunt capacitor with the FCL. Simulation results showed that the RRRV under all fault modes could be restrained to below the rated value by introducing a certain shunt capacitor.

1 | INTRODUCTION

Short circuit currents increase with the expansion of power systems and an increase in capacity. They threaten the reliability of the system when the short circuit current exceeds the breaking limitation of CBs. Predication research data indicate that the short circuit current at the 500 kV bus in the Pearl River delta in southern China will soon exceed 80 kA if no further current limiting measures are taken [1]. This short circuit current will exceed the breaking capacity of the installed 500 kV CBs with a maximum rated short circuit current of 63 kA. There are several potential methods for solving the problem, such as partition running of the power grid, bus splitting, and developing CBs with larger interruption capacity, but these methods will reduce the reliability and flexibility of power system or require a large investment [2]. To solve this issue, a research project on a 500 kV economic fault current limiter (FCL) was conducted by Chinese institutes; the project was supported by the National Key R&D Programme of China.

The emerging superconducting FCL is more expensive than the current limiting reactor [3]. The solid-state FCL has good performance with a fast response but is intended for application in a distribution network, and the loss of power electronics should be considered [4, 5]. The single-phase magnetic FCL demands too much ferromagnetic material. The three-phase one saves ferromagnetic material but the insulation of the windings makes it costly in transmission systems [6]. Series or parallel resonance FCLs composed of LC circuits and power electronics need further operational validation [7–10]. The performance of bypassing reactors depend on the reliability of fast switches [11]. It requires the fast switch to interrupt at the first fault current zero in a few milliseconds. All of these FCLs face common challenges such as low economic efficiency and low reliability with respect to high-voltage applications. In recent years, a dry air-core highly coupled split reactor (HCSR) was developed and used to make current distribute evenly in a parallel-connected circuit breaker (CB) for a higher interruption capacity, which was validated in a 252 kV power system [12–18]. Based on the HCSR and fast vacuum switches, our project team proposed a scheme of a new FCL, as shown in Figure 1 [19]. Here, the main focus is on the influence on the interruption process of the main CB (Figure 1) by introducing this type of FCL.

The current limitation is fulfilled by the variation in the impedance of the HCSR. As shown in Figure 1a, fast switch S

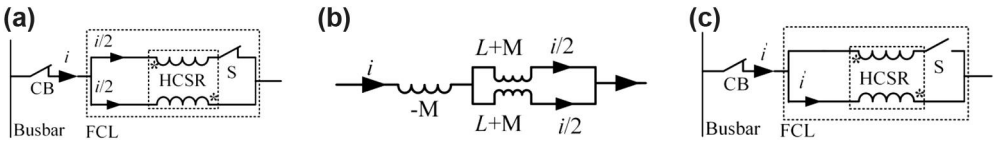

FIGURE 1 Scheme of the proposed fault current limiter (FCL). i, unlimited current; i': limited current. (a) Coupled state with very low impedance; (b) Equivalent circuit of FCL; (c) Decoupled state with large impedance. CB, circuit breaker of the power system, HCSR, highly coupled split reactor

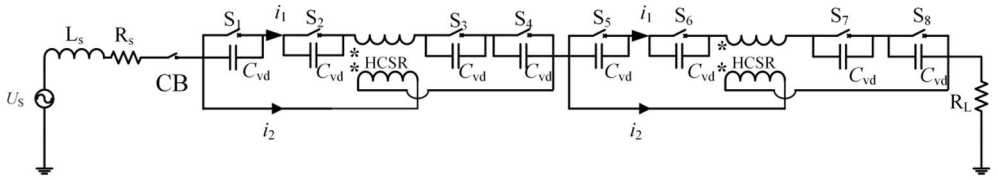

FIGURE 2 Detailed scheme of 500 kV fault current limiter in a single-phase circuit. C_{vd}, gradient capacitors

keeps closed to conduct a normal current. The two branches of HCSR are highly coupled under this condition. Figure 1b is the equivalent circuit of the coupled HCSR. Here, L is the self-inductance of each branch and M is the mutual inductance of the two branches. Ideally, if $M = L$, the equivalent inductance of the FCL is zero. In our case, $M > 0.97\ L$ so the FCL is of low leakage inductance.

In Figure 1c, when a short circuit fault occurs, fast switch S breaks one branch of the HCSR, which leads to decoupling of the two branches. It is known from Figure 1b that the equivalent inductance of the FCL becomes L, which is significantly high and will be in series with CB. The relatively high inductance L can effectively limit the fault current.

Power loss of the FCL consists of two sources. One source is the resistive power loss of the HCSR. The other is power loss of the fast switches, which can be neglected because the contact resistance of the vacuum interrupter is on the order of several of microohms. The design of the 500 kV HCSR indicates a resistance of 3.4 mΩ, which consumes 0.006% of transmitted power if the rated current is 4 kA.

The main contribution of this work is an analysis of the influence on the engineering application of the proposed HCSR-based FCL. The method of varying impedance of the proposed FCL to limit current is different from other types of FCL. The work especially focuses on the impact of the type of FCL on the interrupting procedure of CB. Based on the analysed results, a method to eliminate the negative influence is proposed. In general, inductive FCL and series reactors can influence the interrupting procedure of the CB in series with them [20–22]. The impact of the series reactors on relative projects in China have been studied by other researchers [23–25], but the severity of the interruption in the literature is very different from the work presented here. This research uses a model including an equivalent resistance of the transmission lines to analyse the problem and explain the reason for the differences. The model is further used in asymmetrical three-phase short-circuit faults and short-line faults (SLFs), which have not been investigated before.

2 | INTERRUPTION PROCESS ANALYSIS WITH THE NEW FAULT CURRENT LIMITER

The current limitation procedure of the FCL is presented and the mathematical analysis depending on a single-phase equivalent circuit is conducted in this chapter to find its impact on the interruption process of the CB. Previously, the structure and principle of the 500 kV FCL were introduced, but only briefly.

2.1 | Topology of 500 kV FCL

The topology of the proposed 500 kV FCL based on HCSR and fast switches is shown in Figure 2. There are two identical modules, each of which is 4.1 mH in the current limiting mode. The reason for using two series modules instead of one 8.2-mH FCL is the manufacturing limitation of a single HCSR module. By using two modules, the dimension of the HCSR can be reduced and the insulation design of each module will be easier.

2.1.1 | Fast switches

As shown in Figure 2, four vacuum interrupters are used in each FCL module. S_1 and S_2 make up a fast breaker with double breaks. The fast breaker is driven by an electromagnetic repulsion mechanism. The interrupters can open to 10 mm in 3 ms to commutate the fault current quickly to the lower branch. Once the fast breakers isolate the upper branch, the FCL switches from the current-conducting mode to the current limiting mode.

The rated voltage of each vacuum interrupter is 40.5 kV. There are four interrupters in each FCL module to ensure transient interruption voltage (TRV). The interruption process of the vacuum interrupters will not be discussed here. Gradient capacitors are used to distribute voltage evenly among the eight interrupters.

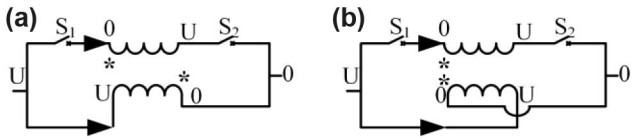

FIGURE 3 Optimization of connection method. (a) Inlet terminals on the same side; (b) Inlet terminals on opposite sides

2.1.2 | Highly coupled split reactor

There are two different methods for connecting the HCSR with the fast switches, as shown in Figure 3 [26]. In Figure 3a, the upper branch is disconnected by S_1 and S_2. The limited current flows through the lower branch and voltage drop U is across the lower branch. Because of mutual inductance $M \approx L$, voltage drop U is also induced across the upper branch, but in an opposite direction. This results in potential difference U between the two branches. By changing the connection method to Figure 3b, voltage between the branches is reduced to zero under ideal circumstances. It benefits insulation between the two branches, especially when they are close to each other to be highly coupled.

The coefficient of mutual induction of the HCSR is designed to be larger than 0.97. In the severest fault condition, the FCL is anticipated to limit a prospective 90 kA short circuit current to 54 kA so that a 500 kV CB with a rated short circuit current of 63 kA can interrupt this limited fault current.

2.2 | Fault current limitation and interruption process

The response of the FCL is presented in Figure 4. In a normal conducting mode, all fast switches keep closed and current flows through both branches of the HCSR. The FCL is in its low inductance state. Provided the fault current starts at t_1, a fast detection system will recognise the fault in at most 3 ms and then it gives orders to the fast breakers. At moment t_2, the contacts start to separate. At current zero t_3, once the arc of the fast breakers is quenched all of the fault current will be transferred to the other branch. This results in a decrease of the fault current, which helps the 500 kV CB interrupt the limited fault current.

After interruption of the fault current by CB, the TRV with a high rate of rise of recovery voltage (RRRV) appears as depicted by the solid line in Figure 5. The TRV curve with the FCL installed apparently exceeds the T100 envelope of 500 kV CBs specified in IEC 62,271-100 [27]. The TRV curve in Figure 5, which excludes the FCL, neglects the reflected wave owing to the discontinuity of the transmission lines. However, the curves are effective to illustrate the differences in the RRRV caused by the FCL. As for the influence on the peak value of the TRV, Figure 5 shows that after moment t_2, the oscillation component (which will be discussed with a single-phase equivalent circuit) decays to nearly zero and does not increase the peak value of the inherent TRV.

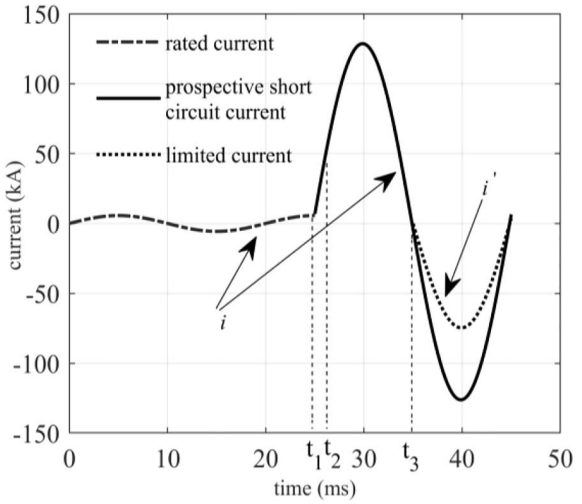

FIGURE 4 Current waveforms under different circumstances. i, current before fast switches interrupt; i', current after fast switches interrupt, t_1, short circuit fault occurs, t_2, fast switches responds, t_3, fault current limiter turns into high impedance

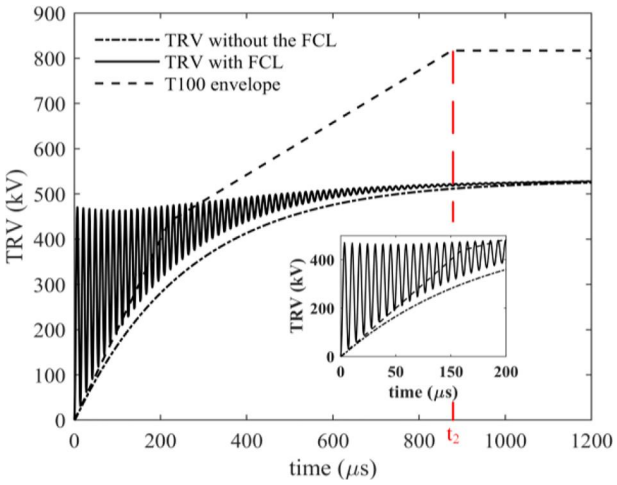

FIGURE 5 TRV under different conditions compared with standardized envelope. TRV, Transient interruption voltage

2.3 | Analysis of TRV on CB

Naef used equivalent circuits composed of resistance, inductance and capacitor (RLC) circuit to study the characteristics of RRRV under a short circuit fault, SLF, and other typical faults in both single-phase and three-phase circuits [28]. The resistance Z_t in Naef's models represents the surge impedance of the parallel transmission lines on the bus. The same method was adopted by other researchers [29]. The calculation formula of TRV derived from the RLC circuit is valid before the reflection wave arrives at the bus and is of considerable accuracy. This period lasts about 1000~2000 μs, which covers the most important first cycle of the high-frequency component of the TRV. A parallel LC circuit is used as a simplified autotransformer model to calculate the TRV of the CB when a short circuit fault happens at the bus on the low-voltage side [30]. The

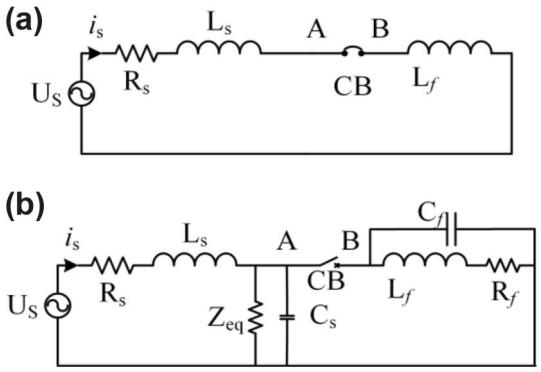

FIGURE 6 Single-phase equivalent circuit for rate of rise of recovery voltage formula deduction when (a) circuit breaker (CB) closes, (b) CB opens

calculation is verified by a simulation based on detailed power grid models. We adopt the method of deriving the RLC equivalent circuit mentioned before to analyse the influence on RRRV caused by the 500 kV FCL. Compared with a detailed power grid model, a simplified RLC circuit can explain the phenomenon clearly and is convenient for theoretical analysis.

Suppose the 500 kV FCL is installed in a three-phase symmetrical circuit, in which a three-phase line to ground short circuit fault happens. The prospective symmetrical short circuit current before the FCL works is 90 kA. The time constant of the short circuit loop is 75 ms, as specified in the standard [27]. Considering the symmetry in the three-phase circuit, a single-phase equivalent circuit, as shown in Figure 6, is used to establish equations.

L_f in Figure 6 represents the total inductance of the FCL after fast switches interrupt current i_1 successfully. C_f is the parasite capacitance of the FCL if there is no extra capacitor. The value of C_f varies from several to tens of nF [20–22]. CB is the 500 kV CB in series with the FCL in the main circuit. A and B represent the two terminals of CB. The 500 kV power system is an effectively earthed neutral system so that the first-pole-to-clear factor is 1.3. In other words, the voltage source is $U_s = 375$ kV. Other parameters of the circuit components are listed in Table 1, in which R_s and L_s are calculated according to the prospective short circuit current and the time constant. The distribution parameters on the system side are replaced by the C_s and Z_{eq}. Z_{eq} is a resistance equal to the equivalent surge impedance of the transmission lines connected to the bus. This resistance attenuates the high-frequency oscillating component of the TRV, as does the transmission line. The 500 kV FCL will be installed at one substation of China Southern Power Grid Company. Five transmission lines are parallel connected to the bus at this station and the short circuit current of a terminal fault at this station is 40 kA. In the future, the short circuit current can reach 90 kA. Assuming that at that time the number of parallel transmission lines connected to the bus increases proportionally to the increased short circuit current, the equivalent resistance is:

$$Z_{eq} = Z_t/n = 40\Omega \tag{1}$$

where Z_t = 450 Ω is the surge impedance of a 500 kV transmission line and n is the number of transmission lines

TABLE 1 Parameters of equivalent circuit

Circuit Parameters	Value
R_s	0.136 Ω
L_s	10.2 mH
Z_{eq}	40 Ω
C_s	3.69 μF
L_f	8.2 mH
R_f	89 Ω
C_f	0.6 nF (inherent value)

connected to the bus. C_s is the equivalent capacitance on the bus side of CB. It is the sum of concentrated capacitors installed at the station and the capacitance of transmission lines to ground. In total, it is 3.69 μF.

When CB is closed, the voltage drop on R_s and current flowing through C_s and C_f are relatively low, so they can be neglected. Then, the circuit is regarded as an inductive circuit of L_f and L_s in series. Voltage U_S should reach peak value at the moment that current crosses zero. At this moment, the voltage of terminal A and B, u_A and u_B are:

$$u_A|_{t=0} = u_B|_{t=0} = u_f(0) = \frac{\sqrt{2}U_s L_f}{L_f + L_s} \tag{2}$$

where $u_f(0)$ represents the voltage drop on the FCL at the current zero moment.

After CB breaks, the circuit is split into two circuits. On the source side of CB, because $0.5\sqrt{(L_s/C_s)} < Z_{eq}$, there is an underdamped oscillation. The oscillation decays rapidly owing to the large resistance of Z_{eq}. On the FCL side of CB, resistance R_f is an equivalent parameter derived from the frequency response of the FCL. It differs very much from the inherent resistance R_{loss} of the FCL, which is of several microohms, whereas R_f is of tens of ohms. R_{loss} leads to power losses when the FCL conducts current, whereas R_f leads to reduced amplitude of TRV on the FCL side of CB.

Regarding the source side circuit, second-order differential Equation (3) can be derived assuming the source voltage to be a constant in a short duration. Relatively small resistance R_s is neglected:

$$\sqrt{2}U_s = L_s C_s \frac{d^2 u_A}{dt^2} + \frac{L_s}{Z_{eq}} \frac{du_A}{dt} + u_A \tag{3}$$

The solution of Equation (3) with time t as the independent variable is:

$$u_A(\alpha_1) = \sqrt{2}U_s \left[1 - ke^{-d_p\alpha_1}\left(\frac{d_p}{\sqrt{1-d_p^2}}\sin\sqrt{1-d_p^2}\alpha_1 + \cos\sqrt{1-d_p^2}\alpha_1\right)\right] \tag{4}$$

where $\alpha_1 = t/\sqrt{(L_sC_s)}$, $k = L_s/(L_s + L_f)$ and $d_p = 0.5\sqrt{(L_s/C_s)}/Z_{eq}$.

Regarding the FCL side circuit, the differential equation is (5):

$$\frac{d^2u_B}{dt^2} + \frac{R_f}{L_f}\frac{du_B}{dt} + \frac{1}{L_fC_f}u_B = 0 \tag{5}$$

Combined with the initial condition given by Equation (2), the solution to Equation (5) is simplified as Equation (6):

$$u_B\left(\alpha_2\right) = \sqrt{2}U_s\left(1-k\right)e^{-d_s\alpha_2}\left(\frac{d_s}{\sqrt{1-d_s^2}}\sin\sqrt{1-d_s^2}\alpha_2 + \cos\sqrt{1-d_s^2}\alpha_2\right) \tag{6}$$

where $d_s = R_f/(2\sqrt{[L_f/C_f]})$ and $\alpha_2 = t/\sqrt{(L_fC_f)}$.

The TRV of CB, u_{AB}, is attained by subtracting u_B from u_A:

$$\begin{aligned} u_{AB} &= u_A - u_B \\ &= \sqrt{2}U_s\left[1 - ke^{-d_p\alpha_1}\left(\frac{d_p}{\sqrt{1-d_p^2}}\sin\sqrt{1-d_p^2}\alpha_1 + \cos\sqrt{1-d_p^2}\alpha_1\right) - \left(1-k\right)e^{-d_s\alpha_2} \times\left(\frac{d_s}{\sqrt{1-d_s^2}}\sin\sqrt{1-d_s^2}\,\alpha_2 + \cos\sqrt{1-d_s^2}\,\alpha_2\right)\right] \end{aligned} \tag{7}$$

The waveforms of u_{AB} and its two components are shown in Figure 7. At first, a capacitance of 0.6–600 nF is given to C_f. The value 0.6 nF is considered to be the inherent parasite capacitance of HCSR. Larger values include an extra shunt capacitor introduced on purpose to suppress the RRRV on the FCL side. It can be seen in Figure 7a that the frequency of the oscillation on the FCL side of CB is much higher than the oscillation on the source side of CB. Before source side voltage u_A reaches its peak value, damped voltage u_B has gone through several cycles. Under this circumstance, the RRRV depends on the rising rate of the first half cycle of u_B. When the total shunt capacitance increases more, for example, C_f = 600 nF, the frequency of voltage u_B decreases and the negative peak value of u_B also reduces owing to larger d_s in Equation (6), which is important to maintain the composited TRV not to exceed the T100 envelope. Figure 7b shows the TRV with C_f = 600 nF and the T100 envelope. The RRRV is reduced

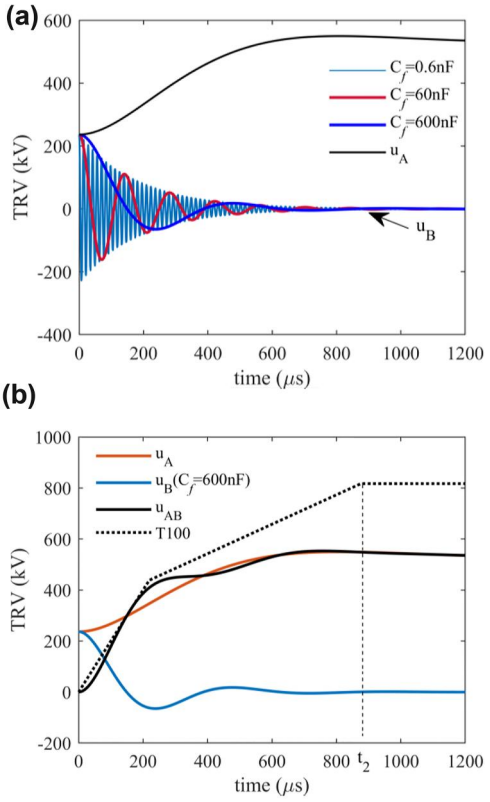

FIGURE 7 Waveforms of transient interruption voltage (TRV) and its components when C_f varies. (a) u_B (coloured lines) and u_A, (b) TRV curves with C_f = 2.5 μF

excessively by a delay in the first negative peak of u_B, but the first peak value of u_{AB} may still exceed the T100 envelope because of an increase in u_A. The shunt capacitor should be chosen carefully to avoid both high RRRV and high voltage. In addition, Figure 7 proves that u_A has almost no influence on RRRV whereas u_B has a dominant effect. It also reveals that the heavily damped u_B will not influence the peak value of TRV after t_2. The adopted circuit model is effective for analysing the RRRV.

It takes u_B half a cycle to reach its first peak value. At this instant of t_p, the TRV reaches a local maximum:

$$t_p = \pi\sqrt{L_fC_f}\Big/\sqrt{1-d_s^2} \tag{8}$$

Replace variable t in Equation (7) with Equation (8), the RRRV after simplification is:

$$RRRV = \frac{1}{t_p}\left[u_A\left(\frac{t_p}{\sqrt{L_sC_s}}\right) - u_B\left(\frac{t_p}{\sqrt{L_fC_f}}\right)\right] \tag{9}$$

Take the parameters of the circuit on the source side of CB as constants, only L_f and C_f affect the RRRV. The specific influence of these two parameters is discussed next.

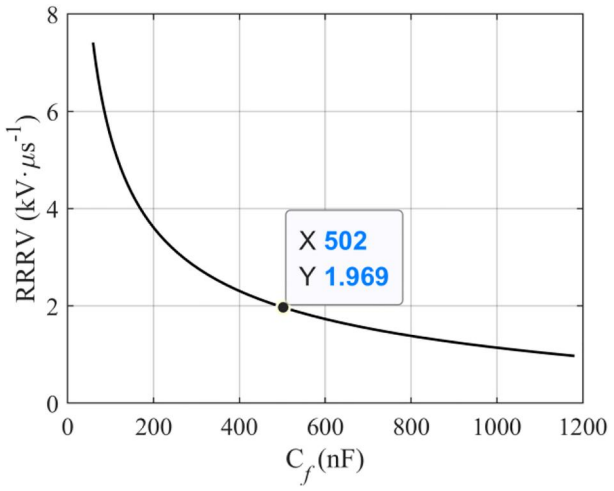

FIGURE 8 Relation between and shunt capacitance. RRRV, rate of rise of recovery voltage

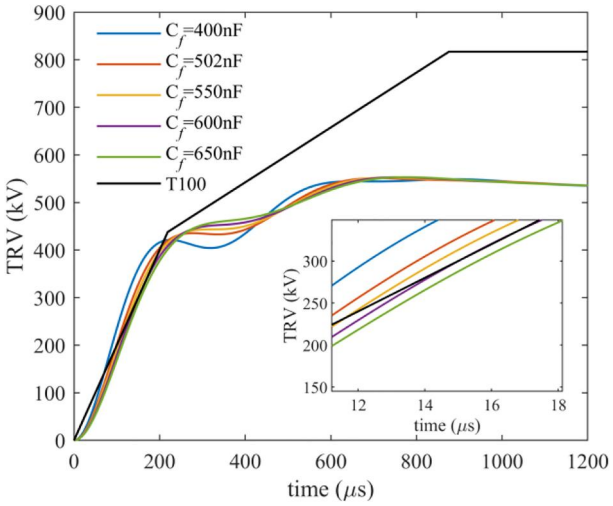

FIGURE 9 Suppressed TRV with different C_f. TRV, transient interruption voltage

2.4 | RRRV suppression by shunt capacitance

The self-inductance of each branch of the HCSR in the 500 kV FCL module is 4.1 mH. When they are in the current limiting mode, the two lower branches are in series so that inductance L_f in Figure 6 is 8.2 mH in total. Substitute variables in Equation (9) with known values and the relation between RRRV and C_f can be described by the curve in Figure 8. The RRRV decreases more slowly with an increase in C_f. When C_f is larger than 502 nF, the calculated RRRV is less than 2 kV/μs. However, as mentioned, some parts of the TRV curve may exceed the T100 envelope. The TRV curves with C_f varying from 400 to 650 nF are plotted in Figure 9. When C_f is 600 nF, the T100 envelope curve is almost tangential to the TRV curve. TRV curves with a shunt capacitor larger than 600 nF are always below the T100 envelope. This infers that the shunt capacitor should be at least 600 nF to ensure that the RRRV does not exceed 2 kV/μs, as shown in Table 2.

2.5 | Non-linear influence of inductance of fault current limiter on rate of rise of recovery voltage

A capacitor larger than 600 nF is needed to suppress the excessive RRRV in the 500 kV FCL project in terms of calculations based on the equivalent circuit. However, in other 500 kV series reactance projects in China, much smaller capacitors, 35~60 nF, are needed [23–25]. The big difference between the impedance of the FCL and series reactance suggests that impedance is why different shunt capacitors should be chosen. The impedance of the 500 kV FCL and the series reactance are compared in Table 3. The limited fault current and the rated RRRV related to breaking current are listed for comparison.

To find the influence of the inductance of the FCL on RRRV with Equation (9), C_f is fixed to 60 nF, which is the shunt capacitance chosen in a series reactance project [25]. The L_f-RRRV curve is plotted in Figure 10. The curve indicates that if inductance L_f is close to the equivalent inductance on the source side, RRRV will be around the peak value. The inductance of the 500 kV FCL in series with the circuit is 8.2 mH, whereas the equivalent inductance of the voltage source is 10.2 mH. When L_f is 8.2 mH, the RRRV is 5.9 kV/μs, around the peak of the L_f-RRRV curve. When L_f is 10 times larger than 8.2 mH, which is the inductance of the series reactance in the literature [23–25], the RRRV decreases to 4.2 kV/μs. As a result, the 500 kV FCL requires a larger shunt capacitor.

On the other hand, for a 500 kV breaker with a rated breaking current of 63 kA, the high impedance series reactance limits the fault current to less than 60% of the rated breaking current. The upper limitation of RRRV under this circumstance is 5 kV/μs. However, in the situation of the 500 kV FCL, a short circuit current is limited to 54 kA, still larger than 85% of the rated breaking current of the CB. The applicable RRRV value should be 2 kV/μs. This lower RRRV requires a larger shunt capacitor.

3 | SIMULATIONS OF FAULTS IN A THREE-PHASE CIRCUIT

This analysis is based on the interruption of a symmetrical limited short-circuit current accompanied by the peak voltage of the power source. In practice, however, the FCL is active to limit the fault current to no more than 20 ms. A three-phase fault (TPF) will induce asymmetrical fault current at the beginning. Before the DC component of the fault current decays to negligible (20 ms is less than the assuming time constant 75 ms of the 500 kV system), the insertion of the FCL by sequence in the three phases will induce a second transient

TABLE 2 Rated TRV for 550 kV current breakers

	First-pole-to-clear factor	1.3 (1.5 for T10)		
	DC component	≤20%		
Test type	Short circuit current level	Amplitude factor	Peak value (kV)	Rate of rise of recovery voltage ($kV \cdot \mu s^{-1}$)
T100	100%	1.3	817	2
T60	60%	1.5	876	3
T30	30%	1.53	899	5
T10	10%	0.9 × 1.7	1031	7

Abbreviations: RRRV, rate of rise of the recovery voltage; TRV, transient interruption voltage.

TABLE 3 Comparison of 500 kV FCL project and series reactance projects [23, 24, 25]

Projects	Impedance (Ω)	Breaking current after limitation (kA)	Shunt capacitance (nF)	RRRV ($kV \cdot \mu s^{-1}$)
1. Jiangsu Shipai	28	13.35	≥35	<5
2. Shanghai Sijing	14	15.6	60	
3. Guangdong Pengshen	28	11	60	
4. 500 kV FCL	2.5	54	1400	<2

Abbreviations: FCL, fault current limiter; RRRV, rate of rise of the recovery voltage.

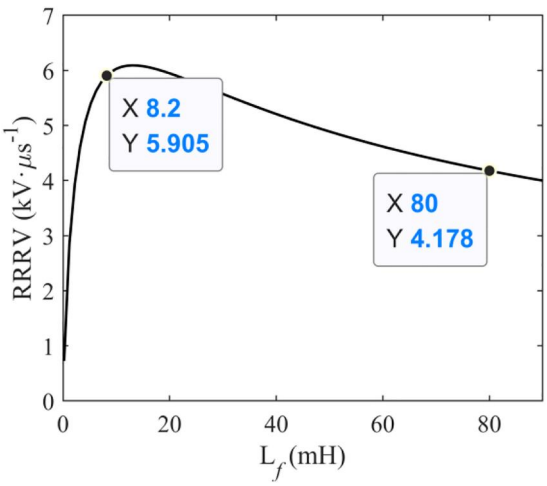

FIGURE 10 Relation between rate of rise of recovery voltage and inductance of fault current limiter

of current and the increased total inductance will make the time constant increase. The 500 kV CB is assumed to break in 50 ms after the fault exists. In such a condition, the voltage of the source at the instant of current zero can deviate from the peak value. In such a case, initial voltage drop $u_f(0)$ on the FCL will be lower than Equation (2). A lower $u_f(0)$ in Equation (7) indicates lower TRV. An analysis of a TPF is helpful to see the influence of an asymmetrical fault current.

This section takes the terminal fault and SLF as examples, setting up a three-phase circuit simulation model in PSCAD/EMTDC. The simulation model in Figure 11 includes the equivalent circuit of the power system, in which resistance Z_{eq} represents the effect of transmission lines. The FCL model is switched to Figure 6b after it is activated. A resistor is added as the load.

To suppress the RRRV, the shunt capacitor can be configured either between the FCL and the earth, like C_e, or across the FCL, like C_p in Figure 11. As for a low-rated voltage system, both shunt capacitors C_e and C_p are used. However, in a 500 kV and above system, C_e should meet the tough requirement of insulation to the earth, whereas C_p only needs to endure the voltage drop on the FCL, and this voltage drop is low under normal conditions. The simulation chooses to use only C_p in the 500 kV system.

The conditions set for the simulation are:

(1) The rated current of the FCL is 4000 A;
(2) The rated short circuit current of a fault at the load side of the FCL is 90 kA;
(3) The time constant of the DC component of the short circuit current is 75 ms according to the literature [27].

The values of the circuit components are calculated with these conditions. A list of the entire parameters adopted in the simulation is in Table 4; they are calculated on the condition of a rated short circuit current fault. The equivalent circuits of the source side related to T10~T60 are derived by the method introduced in Peelo [32].

The proposed FCL will keep being activated because it is triggered by the control and protection system. In such a case, the 500 kV CB will reclose and rebreak with the FCL as an inductive load. A simulation is carried out to investigate the TRV and the current interruption process when considering the reclosing operation of a CB. This simulation is assumed to interrupt a 90 kA prospective short circuit current with the

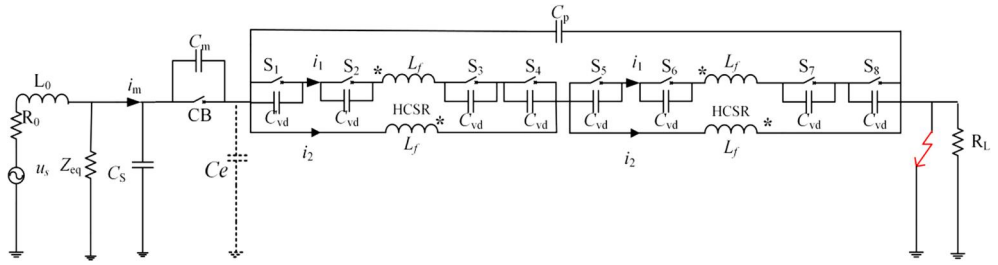

FIGURE 11 Single-phase diagram of the three-phase circuit simulation model. CB, circuit breaker; HCSR, highly coupled split reactor

TABLE 4 Values of components in a rated short circuit current fault simulation model

	Component	Value
1. Equivalent circuit of power system	L_0	10.2 mH
	R_0	0.136 Ω
2. Line to ground branch	C_s	3.69 μF
	Z_{eq}	40 Ω
3. Single module of 500 kV FCL	L_f	4.1 mH
	Coefficient of mutual inductance	0.97
	C_{vd}	800 pF
4. 500 kV circuit breaker	C_m	1000 pF [31]

Abbreviation: FCL, fault current limiter.

FCL. The circuit configuration is the same as the T100 terminal fault.

The SLF is of special concern because of the high initial RRRV. The influence of the FCL in an SLF should be investigated. A simulation is carried out for SLF after the FCL is installed at the line side of the 500 kV CB. The circuit model for simulation is shown in Figure 12. The transmission lines in the module are quadruple-split, steel-reinforced aluminium conductors. The spaces between the lines and the geometrical parameters of the transmission lines are set up according to actual 500 kV transmission lines [33]. The length of lines is 952 m for L_{90} and 1785 m for L_{75}, according to Appendix A in Iec 62271-100 [27]. L_{90} shows that the SLF current is 90% of the rated breaking current of a breaker. The meaning of L_{75} is similar. Standard TRV parameters under an SLF of 550 kV breakers are shown in Table 5.

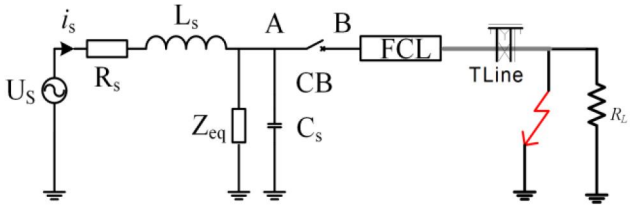

FIGURE 12 Simulation module for short-line fault

TABLE 5 Standard transient interruption voltage parameters under short-line fault

Test Parameter	Test type	Value
First peak value of TRV	L_{90}	81.6 kV
	L_{75}	128.5 kV
RRRV of line side	L_{90}	11.3 kV μs^{-1}
	L_{75}	9.4 kV μs^{-1}
RRRV of source side	L_{90}	1.8 kV μs^{-1}
	L_{75}	1.5 kV μs^{-1}

Abbreviations: RRV, Rate of rise of recovery voltage; TRV, transient interruption voltage.

4 | DISCUSSION ON SIMULATION RESULTS

4.1 | Terminal fault

The simulation considers a TPF and a single-phase fault (SPF). In general, the interruption condition in a TPF is more severe than a two-phase fault, but sometimes an SPF can be more severe than a TPF. Therefore, the shunt capacitance needed in a TPF is investigated first. Then, the capacitance value is verified in an SPF. The 90 kA fault current is limited to 54 kA by the FCL and the 500 kV CB has a rated short-circuit current of 63 kA. In such a case, the TRV envelope of T100 is chosen for comparison.

The TRV curves with 600 nF in Figure 13 have RRRVs lower than 2 kV/μs, which is also applicable for T10∼T60. The TRV given by Equation (7) has two independent components. The TRV parameters of T10 to T60 require only

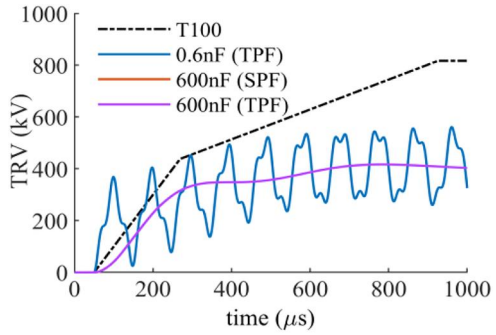

FIGURE 13 TRV in TPF and SPF. TPF, three-phase fault; TRV, transient interruption voltage; SPF, single-phase fault

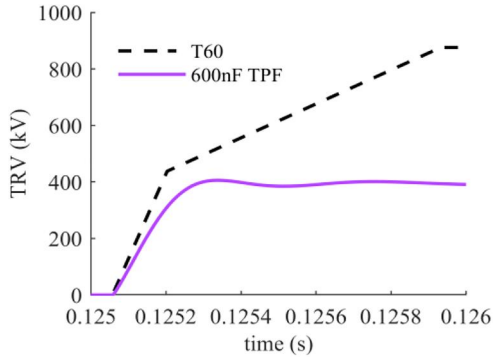

FIGURE 14 TRV curves under T60. TRV, ransient interruption voltage: TPF, three-phase fault

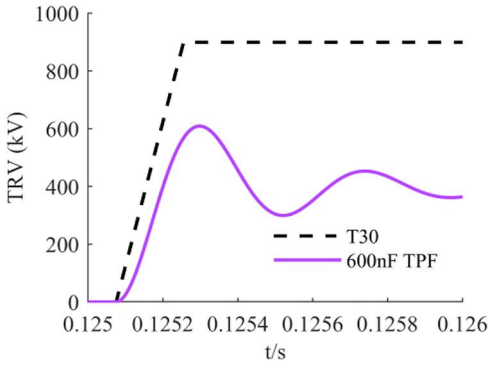

FIGURE 15 TRV curves under T30. TPF, three-phase fault; TRV, ransient interruption voltage

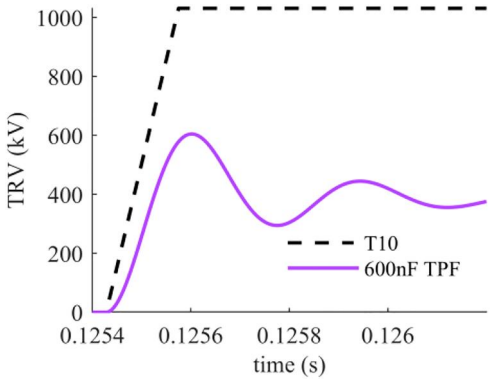

FIGURE 16 TRV curves under T10. TRV, transient interruption voltage; TPF, three-phase fault

modifications of the equivalent circuit of the source side, but the FCL model will remain unchanged. Owing to the lower short-circuit current, the equivalent inductance of the source increases, which means a lower $u_f(0)$ and lower RRRV. As shown in Figures 14, 15 and 16, the TRV curves are derived when the prospective short circuit current is 54, 27 and 9 kA, respectively. Each of these TRV is well below the regulated envelope.

4.2 | Reclosing and rebreaking

The fault current interruption process of the 500 kV CB is extended to include the reclosing and rebreaking operation. The current and TRV waveforms of the first-phase-to-clear are given in Figure 17 and analysed next.

In the lower graph of the current waveform, the dashed black line is the prospective fault current with a steady-state value of 90 kA (r.m.s). The solid red current curve is the result of activating the FCL. During the first half cycle of the fault current, the fast switches open but cannot extinguish the arc until the following current zero comes. The fault current is therefore not limited in the first half cycle. Once the fast switches interrupt successfully at the beginning of the second half cycle, the fault current is limited. The limited fault current is 54 kA (r.m.s), which is 86% of the rated short-circuit current of the 500 kV CB. The simulation assumes the CB isolates the fault in 50 ms. At the instant of the first opening operation, the TRV rises in the upper TRV graph. In the left zoomed view of the time range from 0.125 to 0.127 s, the TRV is well below the T100 envelope.

The reclosing operation is triggered 300 ms after the first opening operation. Until now, the FCL is activated. In this case, after CB recloses, the current will be a limited fault current. The uncleared fault triggers the second opening operation immediately. Again, it takes the CB 50 ms to rebreak. At the second interruption instant, the TRV rises with a steeper rate, as shown in the zoomed view. However, the TRV curve is still under the T100 envelope.

The current waveform around the first interruption and the second one are compared with the source voltage of phase A in Figure 18. I_{sc1} refers to the short-circuit current before the first interruption and I_{sc2} refers to the second one. To make the phase difference between the voltage and the current obvious, the source voltage in cosine expression is shifted 90 degrees to be a sine waveform. At the instant of interruption, I_{sc2} is closer to the peak voltage, which brings about the steeper TRV at the rebreaking instant.

4.3 | Short-line fault

The TRV waveform of an L_{90} SLF is given in Figure 19. The 600 nF shunt capacitor is considered. The triangular waveform

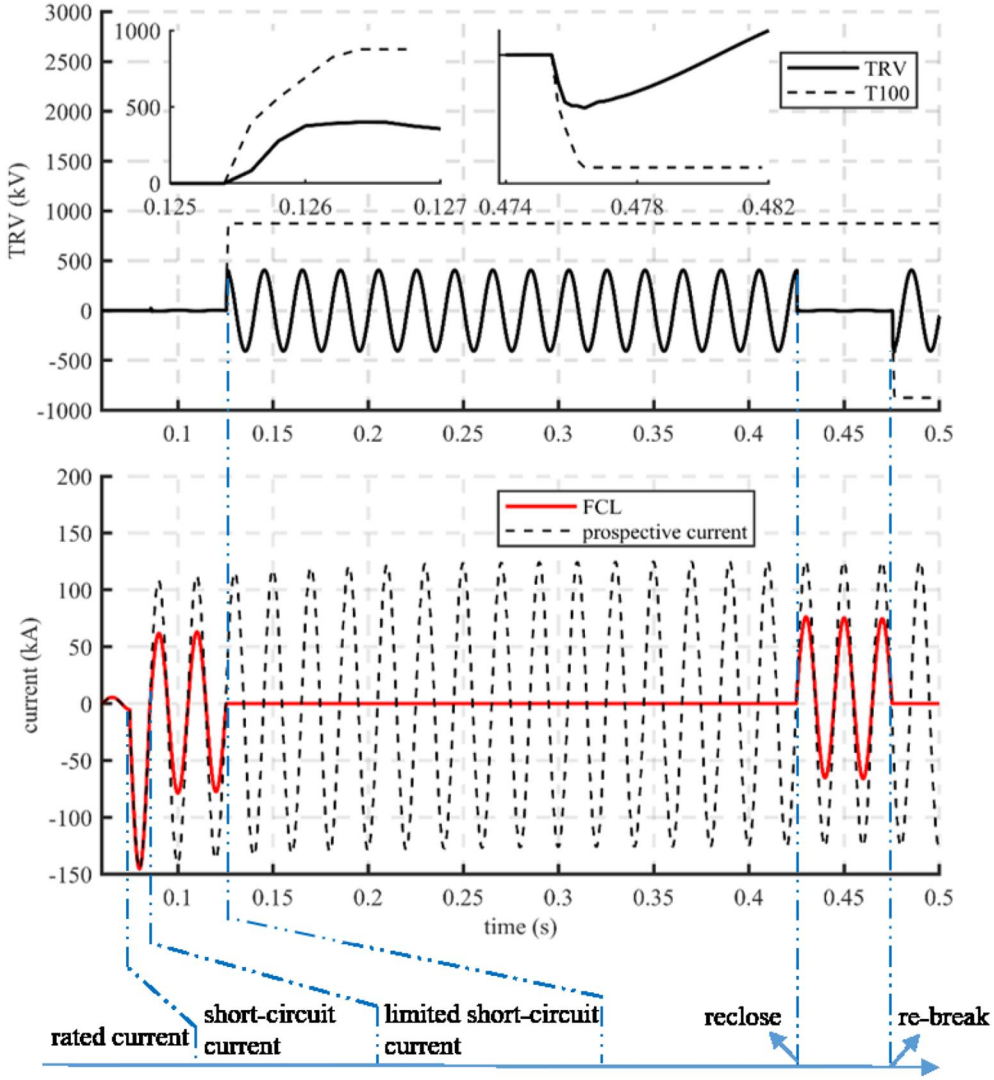

FIGURE 17 Interruption process of reclosing and rebreaking. FCL, fault current limiter; TRV, transient interruption voltage

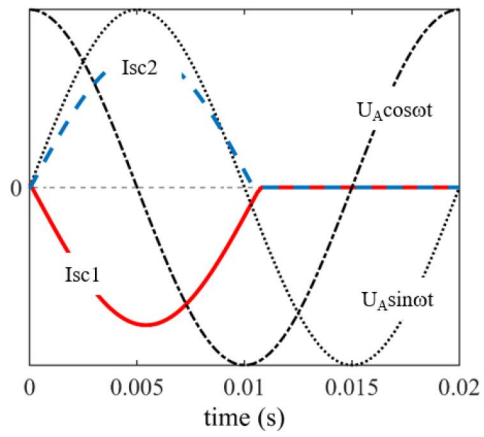

FIGURE 18 Phase difference between the short-circuit current and the source voltage

tagged with u_L is the voltage across the transmission line. Curve u_{FCL} is the voltage across the FCL. Lowest curve u_B is the voltage of terminal B of CB, which is the sum of u_{FCL} and u_L. The last curve TRV is the voltage across the CB. At the instant of current breaking, u_{FCL} is much greater than u_L. This is because the inductance of the FCL is much larger than the short transmission line. If there is no FCL, the source voltage is distributed proportionally to L_s/L_L. L_s and L_L represent the inductance of the power source and the transmission line, respectively. After insertion of the FCL, the source voltage is distributed by $L_s/(L_s + L_L + L_{FCL})$, $L_{FCL}/(L_s + L_L + L_{FCL})$ and $L_L/(L_s + L_L + L_{FCL})$. Consequently, u_L is smaller and the first peak value of the TRV will be reduced. The first peak value of TRV in Figure 19 is 21.6 kV, far less than the regulated value, 81.6 kV. The regulated value is calculated based on a symmetrical current. Again, the simulation results are under the condition of an asymmetrical current. This deviation in

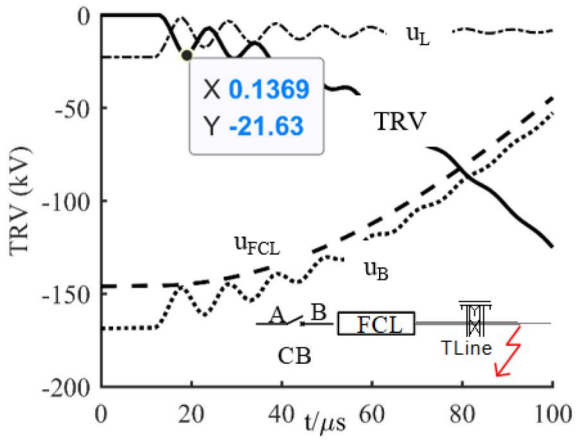

FIGURE 19 Voltage waveforms in an L_{90} short-line fault. CB, circuit breaker; TRV, transient interruption voltage

TABLE 6 TRV parameters under SLF without shunt capacitor connected with the FCL

TRV parameters	Test type	Value
The first peak value of TRV	L_{90}	21.6 kV
	L_{75}	58 kV
RRRV of line side	L_{90}	3.6 kV·μs^{-1}
	L_{75}	4.5 kV·μs^{-1}
RRRV of source side	L_{90}	0.8 kV·μs^{-1}
	L_{75}	0.9 kV·μs^{-1}

Abbreviations: FCL, fault current limiter; RRRV, rate of rise of recovery voltage; SLF, short-line fault; TRV, transient interruption voltage.

symmetry also contributes to the reduced first peak value of the TRV. The result of L_{75} is similar. The TRV parameters in L_{90} and L_{75} SLF are shown in Table 6. Compared with the regulated values in Table 5, the interruption condition with the FCL shunt by a capacitor is within the competence of the CB. This suggests that the influence of the FCL on TRV under an SLF is positive.

4.4 | Insulation coordination of shunt capacitor

The shunt capacitor is installed across the FCL as capacitor C_p, illustrated in Figure 11. The overvoltages that the shunt capacitor should endure under TPF, SPF and SLF are presented in Table 7. The overvoltage under a TPF is the highest. The shunt capacitor can be regarded as short-circuited by the FCL during normal conditions. Hence the overvoltage occurs only when the fault is cleared after the FCL is activated. The peak voltage in Table 7 is the transient voltage after the FCL is activated. In the steady state of a 54 kA fault current, the r.m.s voltage drop will be 54 kA × 2.5 Ω = 135 kV. According to the simulation results and the guide in Iec 60871-1 [34], the rated voltage of 252 kV is chosen for the insulation between shunt capacitor terminals. The terminal to earth insulation level should be 550 kV.

TABLE 7 Overvoltage accounting for shunt capacitor

Fault type		Peak Overvoltage
Short circuit fault	TPF	218 kV
	SPF	218 kV
SLF	L_{90}	174 kV
	L_{75}	156 kV

Abbreviations: SLF, short-line fault; SPF, single-phase fault; TPF, threephase fault.

5 | CONCLUSION

The proposed FCL based on HCSR and fast switches can limit the fault current effectively. These studies show that the RRRV of the CB increases much higher because of the series inductance and inherent capacitance of the FCL. There is a nonlinear relation between the inductance of the FCL and the RRRV. When the inductance of the FCL is close to the equivalent inductance of the power system, the RRRV is around its peak value.

The analytical RRRV assuming interrupting a symmetrical limited short-circuit current is more severe than in practice. In practice, the voltage of source at current zero may deviate from the peak value, which reduces the RRRV. Simulation results indicate that the RRRV of the 500 kV CB can reach 5.1 kV/μs under the three phase-to-phase earth fault.

The RRRV could be effectively suppressed by introducing a 600 nF shunt capacitor C_p across the FCL terminals, as shown in Figure 11. According to the simulation results, the TRVs under all fault modes are below the rated values if a 600 nF capacitor is used. The rated voltage of the capacitor is recommended at 252 V for insulation between terminals and 550 kV for insulation between the terminal and earth.

ACKNOWLEDGEMENTS

This work was supported by the National Key R&D Programme of China under Grant 2018YFB0904300.

ORCID

Qiang Tang https://orcid.org/0000-0002-9880-4781
Shenli Jia https://orcid.org/0000-0003-2782-2234

REFERENCES

1. Hu, T., et al.: Analysis of transient recovery voltage restrictive measures when 500 kV current limiting reactor connected to 90 kA short-circuit current system. Southern Power Syst. Techn. 13(12), 53–59 (2019) (in Chinese)
2. CIGRE Working Group A3.23: Application and Feasibility of Fault Current Limiters in Power Systems, pp. 67–91. CIGRE Tech. Brochure Paris (2012)
3. Castro, L.M., Guillen, D., Trillaud, F.: On short-circuit current calculations including superconducting fault current limiters (ScFCLs). IEEE Trans. Power Deliv. 33(5), 2513–2523 (2018)

4. Radmanesh, H., et al.: A novel solid-state fault current-limiting circuit breaker for medium-voltage network applications. IEEE Trans. Power Deliv. 31(1), 236–244 (2016)
5. Nourmohamadi, H., et al.: A new structure of fault current limiter based on the system impedance with fast eliminating method and simple control procedure. IEEE Trans. Ind. Electron. 65(1), 261–269 (2018)
6. Yuan, J., et al.: A novel three-phase compact saturated-core fault current limiter. IEEE Trans. Magn. 53(11), 1–4 (2017)
7. Radmanesh, H., Fathi, S.H.: Fast AC reactor-based fault current limiters application in distribution network. High Volt. 3(3), 232–243 (2018)
8. Radmanesh, H., Fathi, S.H.: Parallel resonance type fault current limiting circuit breaker. High Volt. 5(1), 76–82 (2020)
9. Radmanesh, H.: Distribution network protection using smart dual functional series resonance-based fault current and ferroresonance overvoltage limiter. IEEE Trans. Smart Grid. 9(4), 3070–3078 (2018)
10. Naderi, S.B., Jafari, M., Tarafdar Hagh, M.: Parallel-resonance-type fault current limiter. IEEE Trans. Ind. Electron. 60(7), 2538–2546 (2013)
11. Chen, X., et al.: Parameter optimization design method for a fast-switch-based fault current limiter and circuit breaker. Int. J. Electr. Power Energy Syst. 114, 105377 (2020)
12. Wang, Y., et al.: Interrupting process simulation of HCSR based 252 kV/85 kA large capacity short-circuit current breaking device. Southern Power Syst. Techn. 11(3), 39–45 (2017) (in Chinese)
13. Su, H, et al.: Influence of parallelled capacitor on parallelled high-voltage SF_6 circuit breakers with highly coupled split reactor. High Volt. Eng. 43(3), 866–871 (2017) (in Chinese)
14. Guo, Z., et al.: Interrupting characteristics of parallelled SF6Circuit breakers with a highly coupled split reactor. IEEE Trans. Compon., Packag. Manufact. Technol. 7(5), 768–776 (2017)
15. Wang, Y., et al.: Simulation study and breakdown characteristics assessment on breaking process of 252 kV/85 kA parallelled short-circuit current breaking device. Guangdong Electric Power. 31(8), 104–110 (2018) (in Chinese)
16. Yuan, Z., et al.: Current dividing process of parallelled circuit breakers with high coupled split reactor. High Volt. Eng. 38(8), 2008–2014 (2012) (in Chinese)
17. Qu, D., et al.: Development of high coupled split reactor for large capacity parallel circuit breaker device. Transformer. 54(7), 25–32 (2017) (in Chinese)
18. Yuan, F., et al.: Optimization design of a high-coupling split reactor in a parallel-type circuit breaker. IEEE Access. 7, 33473–33480 (2019)
19. Chen, C., et al.: Research on the lightning intruding overvoltage and protection measures of 500 kV AC fault current limiter. Energies. 12(20), 3845 (2019)
20. Liu, H., et al.: Impact of the inductive FCL on the interrupting characteristics of high-voltage CBs during out-of-phase faults. IEEE Trans. Power Deliv. 24(4), 2177–2185 (2009)
21. Li, Q., et al.: Impact research of inductive FCL on the rate of rise of recovery voltage with circuit breakers. IEEE Trans. Power Deliv. 23, 1978–1985 (2008)
22. Calixte, E., et al.: Interrupting condition imposed on a circuit breaker connected with fault current limiter. In: Transmission & Distribution Conference & Exhibition: Asia Pacific IEEE/PES, pp. 408–412. Yokohama (2002)
23. Yin, Y., Xie, T., Zhou, Z.: Analysis on breaker TRV for 500 kV lines with series reactors. Jiangsu Electr. Eng. 33(6), 45–47 (2014) (in Chinese)
24. Xue, M., et al.: Application of the first 500 kV series reactors to East China power grid. East China Electric Power. 36(11), 47–50 (2008) (in Chinese)
25. Jia, L., et al.: Study on influence of 500 kV series reactor on interrupting capability of line circuit breaker. Southern Power Syst. Techn. 8(6), 7–11 (2014) (in Chinese)
26. Wu, K., et al.: Voltage distribution analysis of high coupled split reactor in 500 kV AC fault current limiter. IEEE Access. 8, 185804–185815 (2020)
27. IEC 62271-100: High-Voltage Switchgear and Controlgear - Part 100: Alternating-Current Circuit-Breakers, IEC- International Electrotechnical Commission, Geneva (2017)
28. Naef, O., Zimmerman, C.P., Beehler, J.E.: Proposed transient recovery voltage ratings for power circuit breakers. IEEE Trans. Power Appar. Syst. 84(7), 580–608 (1965)
29. Griscom, S.B., Sauter, D.M., Ellis, H.M.: Transient recovery voltages on power systems Part II - practical methods of determination. Trans. AIEE, Part III: Power Appar. Syst. 77(3), 592–604 (1958)
30. Vietor, G.C., Ahrens, P.R., Harper, W.E.: Autotransformer circuit breaker transient recovery voltages associated with interrupting low voltage bus faults. IEEE Trans. Power Appar. Syst. PAS-100(8), 4065–4073 (1981)
31. Wang, Q., Ning, F., Qiu, Y.: Selection of parameters for circuit-breaker capacitors. Power Capacitor. 28(4), 7–10 (2003) (in Chinese)
32. Peelo, D.F.: Current Interruption Transients Calculation, pp. 61–103. John Wiley & Sons, Chichester (2014)
33. Cao B., et al.: Simulation of secondary arc current and recovery voltage for 500 kV transmission line based on PSCAD. High Volt. Appar. 50(12), 71–78 (2014) (in Chinese)
34. IEC 60871-1: Shunt Capacitors for a.c. Power System Having a Rated Voltage Above 1000V—Part 1: General, IEC- International Electrotechnical Commission, Geneva (2014)

How to cite this article: Tang, Q., et al.: Analysis of influence of a novel inductive fault current limiter on the circuit breaker in 500 kV power system. High Volt. 6(6), 997–1008 (2021). https://doi.org/10.1049/hve2.12097